

# Detection and Reduction of Overestimation in Guaranteed Simulations of Hamiltonian Systems\*

Andreas Rauh

Chair of Mechatronics, University of Rostock, D-18059  
Rostock, Germany

`Andreas.Rauh@uni-rostock.de`

Ekaterina Auer

Faculty of Engineering, INKO  
University of Duisburg-Essen, D-47048 Duisburg, Ger-  
many

`Auer@inf.uni-due.de`

Mareile Freihold

Institute of Measurement, Control, and Microtechnol-  
ogy, University of Ulm, D-89069 Ulm, Germany

`M.Freihold@web.de`

Eberhard P. Hofer

Institute of Measurement, Control, and Microtechnol-  
ogy, University of Ulm, D-89069 Ulm, Germany

`Eberhard.Hofer@uni-ulm.de`

Harald Aschemann

University of Rostock, D-18059 Rostock, Germany

`Harald.Aschemann@uni-rostock.de`

## Abstract

In this paper, we introduce a general-purpose approach for the detection and reduction of overestimation in verified interval simulations of the dynamics of mechanical systems. For that purpose, we automatically derive constraints which eliminate physically meaningless parts of the state enclosures of the corresponding ordinary differential equations. The practical applicability of this procedure is demonstrated by a prototypical implementation using the verified solver VALENCIA-IVP. This extension of VALENCIA-IVP is interfaced with SMARTMOBILE, a tool for modeling and simulation of mechanical multibody systems. Simulation results are presented to characterize this new strategy.

**Keywords:** Hamiltonian systems, constraints, consistency tests, VALENCIA-IVP, SMARTMOBILE

**AMS subject classifications:** 65P10, 65G20, 70H07, 70H45

---

\*Submitted: January 19, 2009; Revised: February 9, 2010; Accepted: March 1, 2010.

## 1 Introduction

Dynamics of a large class of mechanical systems, electric circuits, and electromechanical components can be described mathematically by sets of canonical equations based on the Hamiltonian formulation of continuous-time state equations [10,11]. For that purpose, the Hamiltonian  $H(q,p)$ , which represents the sum of the potential and kinetic energy, is introduced. The vectors of generalized coordinates  $q$  and generalized momenta  $p$  are then employed to compute the system dynamics using the corresponding canonical equations.

Since the Hamiltonian expresses the total energy of a dynamical system [5], it can be chosen as a candidate for a positive definite Lyapunov function to analyze the stability of nonlinear systems. In recent years, stability-based techniques for controller design have significantly gained in importance. Therefore, stability analysis is one of the most important applications of the Hamiltonian in control engineering. Further, regions of attraction of asymptotically stable equilibria can be derived with its help. Moreover, it can be shown that the Hamiltonian system representation provides additional information about the dynamics of uncertain systems. This information can be employed efficiently as a constraint in interval-based simulation routines to detect, quantify, and reduce overestimation. For that purpose, a consistency test is developed restricting the set of solutions to physically meaningful areas [2]. A basic interval-based approach which identifies constraints to reduce overestimation in verified simulations of sets of ordinary differential equations (ODEs) has been published in [9].

In this paper, we present a more general procedure to derive Hamiltonian constraints automatically. We describe the implementation of these constraints in VALENCIA-IVP for verified simulation of dynamical systems described by sets of ODEs. Furthermore, we show their application to verified modeling and simulation of multibody systems using SMARTMOBILE [1] with VALENCIA-IVP [7,8] as the underlying ODE solver. In general, similar implementations of physically motivated constraints are possible for any other verified ODE solver. For visualization purposes, we consider a simple example in which the Hamiltonian describes a closed mechanical system without any gain or loss of energy.

In Section 2, the state-of-the-art for modeling of mechanical systems is reviewed with the focus on Hamiltonian system formulations. This type of modeling is used in robotics and other disciplines of engineering to describe dynamical systems for which conservation properties, such as the conservation of energy, hold. In Section 3, a classification of physical constraints which can be employed to tighten the set of possible states of a dynamical system is given. A general-purpose procedure for the detection and reduction of overestimation using the above-mentioned constraints in interval simulations is summarized in Section 4 with the emphasis on Hamiltonian systems. Examples highlighting the use and the efficiency of this procedure are presented in Section 5. Conclusions and an outlook on future research are given in Section 6.

## 2 Modeling of Hamiltonian Systems

As a background for this paper, we summarize the state-of-the-art for mathematical modeling of mechanical multibody systems. Instead of the general state-space representation

$$\dot{x}(t) = f(x(t), u(t), t) \quad (1)$$

with the state vector  $x(t)$  and the control vector  $u(t)$ , such systems are usually described with the help of a minimal set of position and angle variables which are called generalized coordinates  $q = [q_1, \dots, q_s]^T$ .

The generalized coordinates uniquely represent the positions as well as angles of the masses of multibody systems. To systematically choose a set of  $s$  independent generalized coordinates (corresponding to the degrees of freedom of a mechanical system), the Denavit-Hartenberg-conventions are commonly exploited [6]. With the help of the generalized coordinates, the potential energy  $P$  and the kinetic energy  $K$  of a multibody system can be expressed in a straightforward way. As soon as  $P$  and  $K$  are computed, the equations of motion can be derived automatically using either the Lagrangian or the Hamiltonian system representation. Both approaches are common in mechanics since they can be used to represent constraints on the admissible motion of a multibody system and to prove the stability of corresponding control laws [10, 11].

The Lagrangian formulation is given by

$$\frac{d}{dt} \left( \frac{\partial L(q, \dot{q})}{\partial \dot{q}} \right) - \frac{\partial L(q, \dot{q})}{\partial q} = \tau \tag{2}$$

with the Lagrangian  $L = K - P$  defined as the difference of the kinetic energy  $K(q, \dot{q})$  and the potential energy  $P(q)$  as well as the generalized external force vector by  $\tau = [\tau_1, \dots, \tau_s]^T$ .

In contrast, the Hamiltonian  $H = K + P$  is defined as the total energy of a dynamical system, that is, the sum of kinetic and potential energy. In the following, we denote the positive definite, symmetric generalized mass matrix by  $M(q)$  and the generalized momentum vector by  $p = [p_1, \dots, p_s]^T$ .

Using these definitions, the Hamiltonian (cf. [6]) can be expressed by

$$H(q, p) = \frac{1}{2} \cdot p^T \cdot M^{-1}(q) \cdot p + P(q) \tag{3}$$

or equivalently by

$$H(q, \dot{q}) = \frac{1}{2} \cdot \dot{q}^T \cdot M(q) \cdot \dot{q} + P(q) \tag{4}$$

Any Hamiltonian system<sup>1</sup> can be formulated in terms of its corresponding canonical equations. These are the ODEs

$$\dot{q} = \frac{\partial H(q, p)}{\partial p} = M^{-1}(q) \cdot p \tag{5}$$

for the vector of generalized coordinates  $q$  together with the ODEs

$$\dot{p} = -\frac{\partial H(q, p)}{\partial q} + \tau \tag{6}$$

for the generalized momentum vector  $p$ .

Now, the energy balance

$$\frac{d}{dt} H(q, p) = \left( \frac{\partial H(q, p)}{\partial q} \right)^T \cdot \dot{q} + \left( \frac{\partial H(q, p)}{\partial p} \right)^T \cdot \dot{p} = \left( \frac{\partial H(q, p)}{\partial p} \right)^T \cdot \tau = \dot{q}^T \cdot \tau \tag{7}$$

---

<sup>1</sup>A Hamiltonian system is a dynamical system which can be described in generalized coordinates using the expressions  $H(q, p)$  or  $H(q, \dot{q})$  with a positive definite mass matrix  $M(q)$ .

is obtained by differentiation of the expression for the total energy of the system with respect to time. The property

$$\frac{d}{dt}H = 0 \quad (8)$$

holds for  $\tau = 0$ , that is, for conservative systems which are not subject to energy dissipation or external gain of energy. In this system representation, damping is included in the vector  $\tau$ .

A reconstruction of the Hamiltonian representation (5) and (6) from the general state equations (1) is possible if a positive definite, symmetric mass matrix  $M(q)$  which only depends on the generalized coordinates  $q$  can be found. The mass matrix has to fulfill the equations

$$M(q) \cdot \ddot{q} = M(q) \cdot \Phi(q, \dot{q}) \quad \text{with} \quad \frac{\partial \Phi(q, \dot{q})}{\partial \dot{q}_i} = B_i(q) \cdot \dot{q} \quad (9)$$

as well as

$$-\frac{\partial M(q)}{\partial q_i} e_\alpha - \frac{\partial M(q)}{\partial q_\alpha} e_i - M(q) \cdot B_i(q) \cdot e_\alpha + \begin{bmatrix} e_1^T \frac{\partial M(q)}{\partial q_1} \\ \vdots \\ e_s^T \frac{\partial M(q)}{\partial q_s} \end{bmatrix} e_\alpha = 0 \quad (10)$$

for all  $i = 1, \dots, s$  and  $\alpha = 1, \dots, s$ . In (9), the partial derivatives of  $\Phi(q, \dot{q})$  have to be represented as products of matrices  $B_i(q)$  which only depend on  $q$  with the vector of generalized velocities  $\dot{q}$ . In (10), the vectors  $e_i$  and  $e_\alpha$  represent the  $i$ -th and  $\alpha$ -th unit vectors of dimension  $s$ .

In the following, the Hamiltonian and its time-derivative are used to implement a consistency test which identifies and eliminates overestimation in state enclosures determined by verified ODE solvers. The prerequisite for that is the representation of dynamical systems using the canonical equations (5) and (6). These are obtained either directly by modeling or by reformulation of general state-space representations using the conditions (9) and (10).

### 3 Classification of Physical Constraints

Besides constraints which can be derived from the Hamiltonian formulation of dynamical systems, several further types of side conditions exist that can be used in a general simulation framework to restrict the set of solutions to physically meaningful regions.

Such constraints can be classified into holonomic and non-holonomic [3]. Holonomic ones can be expressed as algebraic functions  $g(q, t) = 0$  depending on the time variable  $t$  and the generalized coordinates  $q$ . All other constraints which cannot be represented in this form, for example, inequalities or non-integrable constraints depending on the velocity  $\dot{q}$ , are called non-holonomic.

A typical example for a holonomic constraint is the description of the constrained motion of a (point) mass on the surface of a ball by an algebraic function which depends solely on the generalized coordinates. An example for a non-holonomic constraint is a given bound for the kinetic energy which corresponds to an inequality constraint on the generalized velocities  $\dot{q}$ .

Physical continuity and conservation properties have been studied recently in [2] for a high-dimensional, nonlinear model of human blood cell dynamics [4] to derive constraints for verified simulations.

## 4 Procedure for Detection and Reduction of Overestimation

State enclosures obtained with the help of interval arithmetic in solvers such as VALENCIA-IVP tend to overestimate the true solution set. In [7], the basic approach of VALENCIA-IVP to reduce overestimation in verified simulations of ODEs was presented. The dependency problem in the iteration formula was treated by using mean-value rule evaluation and monotonicity tests instead of naive interval evaluation. Additionally, VALENCIA-IVP can use subdivision strategies for interval enclosures before propagating them to a future point of time. This leads to state enclosures described by the union of usually overlapping interval boxes, see Fig. 1. In general, this enclosure is tighter than the result obtained without subdivision. Thus, the wrapping effect can be reduced and tighter enclosures of the true set of reachable states  $\mathcal{X}_{k+1}$  are computed. Moreover, backward propagation of subintervals from a point of time  $t_{k+1}$  to a previous point  $t_k$  can be used to implement a consistency test which detects intervals originating from overestimation. In this consistency test, three cases are distinguished:

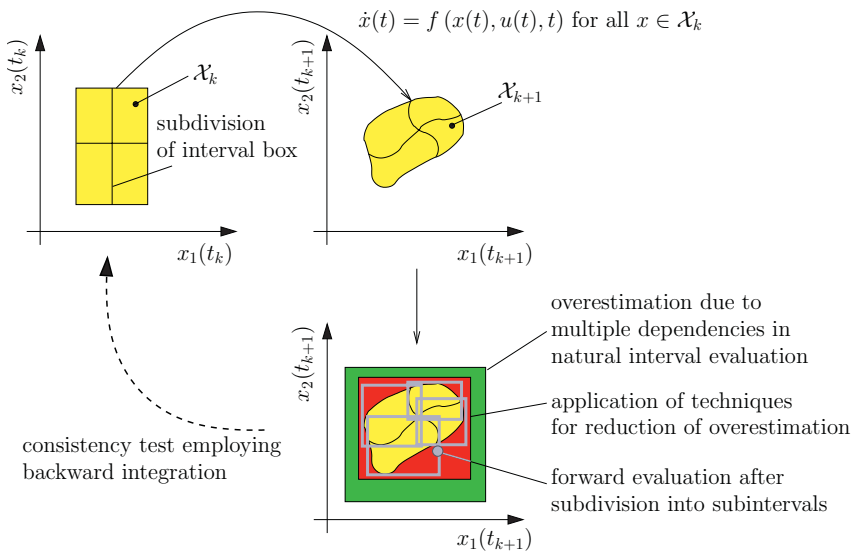


Figure 1: Reduction of overestimation in interval simulations by subdivision of interval boxes in forward and backward evaluation of the state equations.

*Case (A): Subintervals which certainly originate from overestimation.* Such subintervals are deleted. The intersection of the result of the backward integration of these subintervals with the state enclosure of the forward evaluation is empty in at least one component of the state vector for at least one point of time in the time interval  $[t_k ; t_{k+1}]$ .

*Case (B): Subintervals which are consistent with  $[x(t_k)]$ .* These subintervals belong to the solution. Their backward integration leads to time responses which are

completely included in the result of the forward integration for all  $t \in [t_k ; t_{k+1}]$ .

*Case (C): All other subintervals.* Further splitting is required to check consistency.

The drawback of the backward evaluation of the state equations is its computational cost since IVPs have to be solved in a verified way for each subinterval. In this paper, we present a new consistency test which relies mostly on algebraic expressions. It is used before the already existing consistency test by backward integration. The computational effort is reduced significantly with its help because inconsistent subintervals (corresponding to case (A)) are detected prior to the backward integration. Therefore, backward integration is only necessary for subintervals corresponding to case (C) of the new consistency test.

Consider the Hamiltonian system representation summarized in Section 2. The goal is to generate a three-stage sequence

$$\underbrace{q, \dot{q}, M}_{\text{step (1)}} \longrightarrow \underbrace{K, P}_{\text{step (2)}} \longrightarrow \underbrace{H, \dot{H}}_{\text{step (3)}} \quad (11)$$

to derive constraints automatically so that they can be applied in VALENCIA-IVP to detect and reduce overestimation. Step (1) is the description of a dynamical system using generalized coordinates from which an expression for the energy (step (2)) and its time derivative (step (3)) can be formed.

The Hamiltonian of a dynamical system is evaluated in two computationally different but effectively identical ways. First, it is evaluated using the algebraic equations (3) or (4) in which  $q$ ,  $\dot{q}$ , and  $p$  are replaced by the corresponding guaranteed state enclosures. This kind of evaluation is denoted as the Hamiltonian constraint  $H_H$  in the following. Second, the Hamiltonian is evaluated as the solution of an additional ODE by verified integration

$$H_V : \quad H(t) = H(0) + \int_0^t \dot{H}(\tau) d\tau \quad (12)$$

using VALENCIA-IVP. The term  $H(0)$  corresponds to the initial energy of the system. Its guaranteed enclosure is obtained by evaluation of the algebraic expressions (3) or (4) for the corresponding initial state enclosures.

**Step (1):** Find the canonical representation (5), (6) for the given Hamiltonian system.

**Step (2):** Calculate the kinetic energy  $K$  and the potential energy  $P$  with the help of the solution of the canonical equations in step (1). The kinetic energy

$$K(q, \dot{q}) = \frac{1}{2} \cdot \dot{q}^T \cdot M(q) \cdot \dot{q} = \frac{1}{2} \cdot p^T \cdot M^{-1}(q) \cdot p \quad (13)$$

can be computed directly from the information obtained in step (1). It is more difficult to compute a verified enclosure for the potential energy  $P(q)$  if its symbolic representation is not given beforehand. The derivative of  $P(q)$  with respect to the vector of generalized coordinates  $q$  can be expressed by

$$\frac{\partial P(q)}{\partial q} = -\dot{p} - \frac{\partial K(q, \dot{q})}{\partial q} = -\frac{\partial}{\partial q} \left( \frac{1}{2} \cdot p^T \cdot M^{-1}(q) \cdot p \right) + \tau - \frac{d}{dt} \left( M(q) \cdot \dot{q} \right) . \quad (14)$$

The integral of (14) provides the missing expression for the potential energy. To obtain

a complete representation for  $P(q)$ , it is necessary to compute the scalar integrals

$$\begin{aligned}
 P^{<i>}(q) &= \int \left( -\frac{\partial}{\partial q_i} \left( \frac{1}{2} \cdot p^T \cdot M^{-1}(q) \cdot p \right) + \tau - \frac{d}{dt} \left( e_i^T \cdot M(q) \cdot \dot{q} \right) \right) \cdot dq_i \\
 &= \int \left( \frac{1}{2} \cdot \dot{q}^T \cdot \frac{\partial M}{\partial q_i} \cdot \dot{q} + \tau - \frac{d}{dt} \left( e_i^T \cdot M(q) \cdot \dot{q} \right) \right) \cdot dq_i
 \end{aligned}
 \tag{15}$$

for all  $i = 1, \dots, s$ . Using this procedure, we can determine integration constants which possibly depend on  $q_1, \dots, q_{i-1}, q_{i+1}, \dots, q_s$ . The state-independent integration constant representing the reference potential may be chosen arbitrarily without loss of generality.

**Step (3):** Compute the terms  $H$  and  $\dot{H}$ . The interval evaluations of the physically identical constraints  $H_V$  and  $H_H$  are used to detect overestimation by comparing enclosures resulting from different mathematical representations.

To systematically determine the point of time  $t^*$  at which the consistency test should be applied, we define the *reduction area*  $\mathcal{RA}$  in Fig. 2 according to

$$\mathcal{RA}(t) := \text{diam} \{ [H_H(t)] \} - \text{diam} \{ [H_H(t)] \cap [H_V(t)] \} \geq 0 .
 \tag{16}$$

Now, the point of time  $t^*$  in the integration time span  $[t_0; t_f]$  is chosen such that  $\mathcal{RA}(t)$  is maximized. This represents a strategy which helps to detect a maximum amount of overestimation in the consistency test.

To simplify the maximization, the first local maximum of  $\mathcal{RA}(t)$  in the time interval  $t \in [t_0; t_f]$  is used instead of the global maximum. For this point of time, the constraints  $H_V$  and  $H_H$  are mapped back into the original state-space. Then, the Branch and Prune technique is used to eliminate regions which certainly result from overestimation. To illustrate this procedure, we discuss a simple example in the following section. A detailed comparison of six different subdivision strategies as well as criteria for their selection and parameterization can be found in [2].

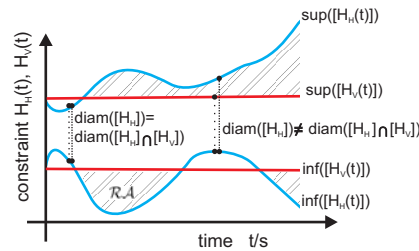


Figure 2: Maximization of the reduction area  $\mathcal{RA}(t)$ .

## 5 Simulation Results

### 5.1 Visualization of the Energy-Based Consistency Test

Consider a simple pendulum consisting of a point mass  $m$  and a massless arm with length  $l$ . The gravitational constant is denoted by  $g$ . The position and velocity of the

point mass are described by

$$\begin{aligned} p_x(t) &= l \cdot \sin(\varphi(t)) & \dot{p}_x(t) &= l \cdot \cos(\varphi(t)) \cdot \dot{\varphi}(t) \\ p_y(t) &= -l \cdot \cos(\varphi(t)) & \dot{p}_y(t) &= l \cdot \sin(\varphi(t)) \cdot \dot{\varphi}(t) \end{aligned} \quad (17)$$

with the angle  $\varphi(t)$  as the generalized coordinate  $q(t)$ . The state-space representation is then given by

$$\dot{q}(t) = \dot{\varphi}(t) \quad \text{and} \quad \ddot{q}(t) = -\frac{g}{l} \cdot \sin(\varphi(t)) \quad . \quad (18)$$

The Hamiltonian is the sum of kinetic and potential energy

$$H(q, \dot{q}) = \frac{1}{2} \cdot m \cdot ((l \cdot \sin(q) \cdot \dot{q})^2 + (l \cdot \cos(q)) \cdot \dot{q})^2) + m \cdot g \cdot (l - l \cdot \cos(q)) \quad . \quad (19)$$

For the initial conditions  $q(0) \in [2.1 ; 2.2]$  and  $\dot{q}(0) \in [3.1 ; 3.2]$ , the optimal point of time  $t^*$  to start the consistency test is identified using maximization of  $\mathcal{RA}(t)$  in (16), see Fig. ?? . Since  $\dot{H}(t)$  has not been simplified symbolically to  $\dot{H} = 0$ , the bounds  $[H_V(t)]$  are not constant. For the point of time  $t^*$ , the state enclosure  $[x(t^*)]$  is split into subintervals. Then, the constraint  $H_H$  is evaluated for each of the subintervals. Intervals which do not overlap with the interval  $[H_V(t^*)]$  are inconsistent and, therefore, eliminated. In Fig. ??, the domains which are inconsistent with the constraints  $[H_V(t^*)]$  and  $[H_H(t^*)]$  before subdivision of  $[x(t^*)]$  are marked by the dotted regions. Additionally, the subintervals of  $[x(t^*)]$  which are kept after the consistency test are depicted. They represent a tight enclosure of the physically consistent domain.

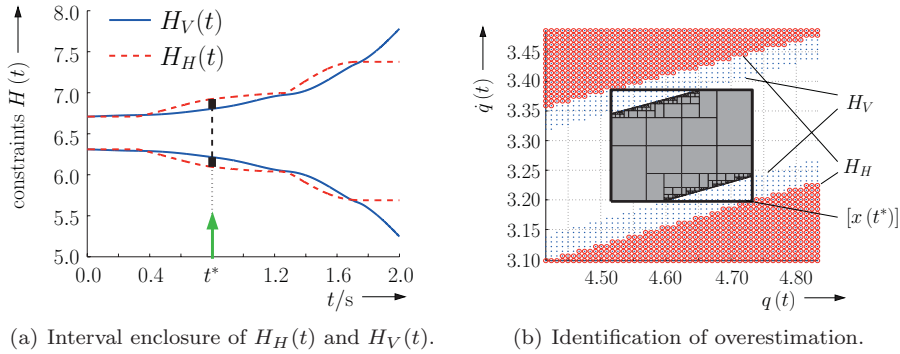


Figure 3: Identification of overestimation using the energy constraint for a simple pendulum with uncertain initial conditions and visualization of the constraint in the  $(q; \dot{q})$ -plane for  $t = t^*$ .

### 5.2 A Double Pendulum

Consider the double pendulum in Fig. 4 as a second application. The positions and velocities of the point masses  $m_1$  and  $m_2$  are given by

$$\begin{aligned}
 p_{x,1} &= l_1 \cdot \sin(\varphi_1) & \dot{p}_{x,1} &= l_1 \cdot \cos(\varphi_1) \cdot \dot{\varphi}_1 \\
 p_{y,1} &= -l_1 \cdot \cos(\varphi_1) & \dot{p}_{y,1} &= l_1 \cdot \sin(\varphi_1) \cdot \dot{\varphi}_1 \\
 p_{x,2} &= l_1 \cdot \sin(\varphi_1) + l_2 \cdot \sin(\varphi_2) & \dot{p}_{x,2} &= l_1 \cdot \cos(\varphi_1) \cdot \dot{\varphi}_1 + l_2 \cdot \cos(\varphi_2) \cdot \dot{\varphi}_2 \\
 p_{y,2} &= -l_1 \cdot \cos(\varphi_1) - l_2 \cdot \cos(\varphi_2) & \dot{p}_{y,2} &= l_1 \cdot \sin(\varphi_1) \cdot \dot{\varphi}_1 + l_2 \cdot \sin(\varphi_2) \cdot \dot{\varphi}_2 .
 \end{aligned}
 \tag{20}$$

The system has  $s = 2$  degrees of freedom. Its generalized coordinates according to the Denavit-Hartenberg-conventions are  $x_1 = \varphi_1$  and  $x_2 = \varphi_2 - \varphi_1$ . Using the state vector

$$x = [x_1 \quad x_2 \quad \dot{x}_1 \quad \dot{x}_2]^T =: [x_1 \quad x_2 \quad x_3 \quad x_4]^T , \tag{21}$$

the double pendulum is described by the ODEs [7]

$$\dot{x} = \begin{bmatrix} 1 & 0 & 0 & 0 \\ 0 & 1 & 0 & 0 \\ 0 & 0 & m_1 l_1 + m_2 (l_1 + l_2 \cos(x_2)) & m_2 l_2 \cos(x_2) \\ 0 & 0 & m_2 (l_1 \cos(x_2) + l_2) & m_2 l_2 \end{bmatrix}^{-1} \cdot \begin{bmatrix} x_3 \\ x_4 \\ -g(m_1 + m_2) \sin(x_1) + m_2 l_2 \sin(x_2) (x_3 + x_4)^2 \\ -g m_2 \sin(x_1 + x_2) - m_2 l_1 \sin(x_2) x_3^2 \end{bmatrix} . \tag{22}$$

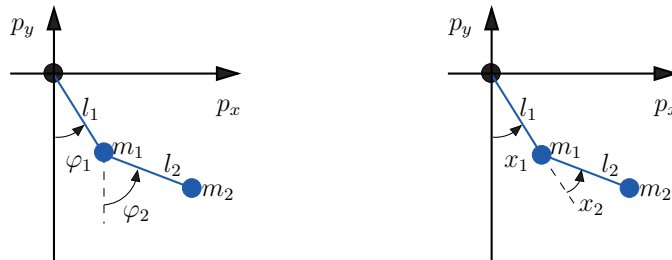


Figure 4: Modeling of a double pendulum with generalized coordinates  $x_1, x_2$ .

Using the procedure described in (9) and (10), the state-dependent, symmetric mass matrix of this system can be reconstructed as

$$M = \begin{bmatrix} (m_1 + m_2) \cdot l_1^2 & m_2 \cdot l_1 \cdot l_2 \cdot \cos(x_2) \\ m_2 \cdot l_1 \cdot l_2 \cdot \cos(x_2) & m_2 \cdot l_2^2 \end{bmatrix} . \tag{23}$$

With this information, the Hamiltonian of the system (corresponding to its total energy) results in

$$H = m_1 \cdot g \cdot p_{y,1} + m_2 \cdot g \cdot p_{y,2} + \frac{1}{2} \cdot m_1 \cdot (\dot{p}_{x,1}^2 + \dot{p}_{y,1}^2) + \frac{1}{2} \cdot m_2 \cdot (\dot{p}_{x,2}^2 + \dot{p}_{y,2}^2) \tag{24}$$

with  $\dot{H} = 0$ . For uncertain initial conditions with

$$\begin{aligned} \inf([x(0)]) &= [0.99 \frac{3\pi}{4} \quad -\frac{11\pi}{20} \quad 0.43 \quad 0.67]^T \text{ and} \\ \sup([x(0)]) &= [1.01 \frac{3\pi}{4} \quad -\frac{11\pi}{20} \quad 0.43 \quad 0.67]^T \end{aligned} \quad (25)$$

state enclosures are computed with the help of VALENCIA-IVP in three different ways. These are:

- (i) numerical modeling of the dynamical system in SMARTMOBILE and simulation without any consistency test (black solid lines in Fig. 5),
- (ii) numerical modeling of the dynamical system in SMARTMOBILE and application of the Hamiltonian constraints (grey lines in Fig. 5), and
- (iii) symbolic modeling of the dynamical system and application of the Hamiltonian constraints in a stand-alone version of VALENCIA-IVP (dashed lines in Fig. 5).

The simulations (ii) and (iii) lead to significantly tighter state enclosures than simulation (i). Both numerical and symbolic modeling approaches give almost identical results with the maximum deviations  $\Delta x_1 = 0.0018$ ,  $\Delta x_2 = 0.0072$ ,  $\Delta x_3 = 0.0066$ , and  $\Delta x_4 = 0.0444$  in the interval diameters of the four state variables which is less than the graphical resolution in Fig. 5. In simulation (ii), the consistency test was applied after at most 0.1s with 10 subdivisions. In simulation (iii), the setting 0.01s for the maximum time between two consistency tests with 50 subdivisions was chosen.

Note that the constraints  $H_V$  and  $H_H$  were not computed symbolically in (ii). To obtain the total energy of the system and, consequently,  $H_H$ , SMARTMOBILE functions `getPotentialEnergy` and `getKineticEnergy` were used. Additionally, the time derivative of their sum was computed by FADBAD++ to provide the basis for  $H_V$ . The result in Fig. 5 demonstrates that the overestimation can be reduced for the numerical approach to modeling of this system as efficiently as for the symbolic one with the help of the new consistency test.

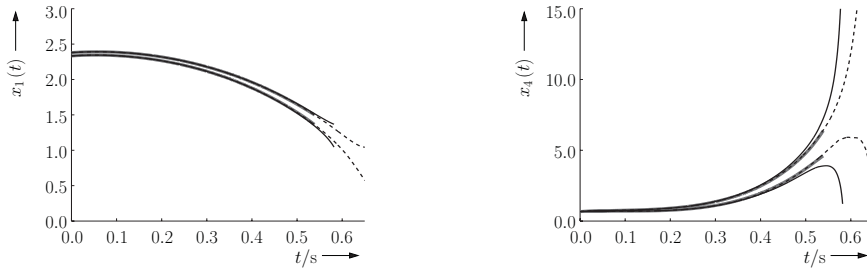


Figure 5: Simulation results for the double pendulum.

## 6 Conclusions and Outlook on Future Research

In this paper, we have presented a general procedure for the derivation and application of Hamiltonian constraints. They are applied to detect and reduce overestimation arising in verified solution techniques for ODEs.

For non-Hamiltonian systems and in situations in which Hamiltonian constraints do not depend on the state variables introducing overestimation, the energy-based constraints might fail to detect a portion of overestimation. To solve this problem, further constraints based on specific physical system properties such as continuity laws or mass balance equations have to be derived. This extension would allow us to generalize the consistency test for use in various applications in engineering, medicine, and biology.

In future work, we will extend the approach for Hamiltonian system formulations for the derivation and verification of stabilizing control laws. In this case, we will focus on systems with non-negligible parameter uncertainties. For many engineering applications, it is difficult to prove asymptotic stability using classical procedures for controller design relying on symbolic formula manipulation if parameter uncertainties have significant influence on the stability of the closed-loop control system. Interval techniques will be used to simplify this task from a computational point of view.

## References

- [1] E. Auer, SMARTMOBILE: *A Framework for Reliable Modeling and Simulation of Kinematics and Dynamics of Mechanical Systems*, PhD thesis, University of Duisburg-Essen, WiKu Verlag Dr. Stein, 2007.
- [2] M. Freihold and E. P. Hofer, “Derivation of physically motivated constraints for efficient interval simulations applied to the analysis of uncertain dynamical systems”, *Intl. Journal of Applied Mathematics and Computer Science AMCS*, vol. 19, no. 3, pp. 485–499, 2009.
- [3] W. Greiner, *Classical Mechanics: Systems of Particles and Hamiltonian Dynamics*, Springer-Verlag, Berlin, 2002.
- [4] E. P. Hofer, B. Tibken, and T. M. Fliedner, “Modern control theory as a tool to describe the biomathematical model of granulocytopoiesis”, In: D. P. H. Möller and O. Richter, editors, *Analyse dynamischer Systeme in Medizin, Biologie, Ökologie*, vol. 275, pp. 33–39. Springer-Verlag, Berlin, 1991.
- [5] B. M. Maschke and A. J. van der Schaft, “Portcontrolled Hamiltonian Representation of Distributed Parameter Systems”, In: N. E. Leonard and R. Ortega, editors, *Proc. of IFAC Workshop on Lagrangian and Hamiltonian methods for nonlinear control*, pp. 28–38, Princeton University, 2000.
- [6] F. Pfeiffer and E. Reithmeier, *Roboterdynamik*, Teubner, Stuttgart, 1987 (in German).
- [7] A. Rauh, E. Auer, and E. P. Hofer, “ValEncIA-IVP: A comparison with other initial value problem solvers”, In: *CD-Proc. of the 12th GAMM-IMACS International Symposium on Scientific Computing, Computer Arithmetic, and Validated Numerics SCAN 2006, Duisburg, Germany*, IEEE Computer Society, 2007.
- [8] A. Rauh, M. Brill, and C. Günther, “A novel interval arithmetic approach for solving differential-algebraic equations with VALENCIA-IVP”, *Intl. Journal of Applied Mathematics and Computer Science AMCS*, vol. 19, no. 3, pp. 381–397, 2009.
- [9] A. B. Singer and P. I. Barton, “Bounding the solutions of parameter dependent nonlinear ordinary differential equations”, *SIAM Journal on Scientific Computing*, vol. 27, no. 6, pp. 2167–2182, 2006.

- [10] A. J. van der Schaft, *Network Modeling and Control of Physical Systems, DISC Theory of Port-Hamiltonian Systems*, 2005  
<http://www.vf.utwente.nl/~schaftaj/downloads-diversen/DISCportbased1.pdf>
- [11] A. J. van der Schaft and B. M. J. Maschke, *Port-Hamiltonian Systems: a Theory for Modeling, Simulation and Control of Complex Physical Systems*, 2003.  
[http://www-lar.deis.unibo.it/euron-geoplex-sumsch/files/lectures.1/Van Der Schaft/VDSchaft.01\\_PCHS.pdf](http://www-lar.deis.unibo.it/euron-geoplex-sumsch/files/lectures.1/Van%20Der%20Schaft/VDSchaft.01_PCHS.pdf)